AIP | Journal of Applied Physics

Micromagnetic simulation of spin-transfer switching in a full-Heusler Co2FeAl0.5Si0.5 alloy spin-valve nanopillar

H. B. Huang, X. Q. Ma, Z. H. Liu, F. Y. Meng, Z. H. Xiao et al.

Citation: J. Appl. Phys. **110**, 033913 (2011); doi: 10.1063/1.3619773
View online: http://dx.doi.org/10.1063/1.3619773
View Table of Contents: http://jap.aip.org/resource/1/JAPIAU/v110/i3
Published by the American Institute of Physics.

Micromagnetic simulation of spin-transfer switching in a full-Heusler $Co_2FeAl_{0.5}Si_{0.5}$ alloy spin-valve nanopillar

H. B. Huang,[1] X. Q. Ma,[1,a)] Z. H. Liu,[1] F. Y. Meng,[1] Z. H. Xiao,[1] P. P. Wu,[1] S. Q. Shi,[2] and L. Q. Chen[3]
[1]*Department of Physics, University of Science and Technology Beijing, Beijing, 100083, China*
[2]*Department of Mechanical Engineering, The Hong Kong Polytechnic University, Hung Hom, Kowloon, Hong Kong*
[3]*Department of Materials Science and Engineering, The Pennsylvania State University, University Park, Pennsylvania 16802, USA*

(Received 16 March 2011; accepted 22 June 2011; published online 10 August 2011)

We investigated the spin-transfer switching in a full-Heusler $Co_2FeAl_{0.5}Si_{0.5}$ alloy spin-valve nanopillar through micromagnetic simulation. A two-step switching hysteresis loop due to the fourfold in-plane magnetocrystalline anisotropy of $Co_2FeAl_{0.5}Si_{0.5}$ layers was obtained. The simulation explains the experimental result of the resistance versus current hysteresis loop and yields good agreement with the measured critical current. Furthermore, the magnetization trajectory and magnetization distribution were shown and analyzed to elucidate the different characters of two-step switching. © *2011 American Institute of Physics*. [doi:10.1063/1.3619773]

I. INTRODUCTION

During the last decade, the spin-transfer torque (STT) effect has attracted a lot of scientific interest after the transfer of spin momentum was predicted[1,2] and observed.[3–6] The spin-transfer torque magnetoresistive random access memory (STT-MRAM) offers superior performance with large storage density, high switching speed, low energy consumption, and avoidance of cross writing. Spin-polarized electrons carry spin angular moments from the fixed layer to the free layer and cause free layer reversal when the current density exceeds a critical current density J_c. A lot of efforts have been made in the reduction of J_c to $\sim 10^7$ A/cm^2,[7–12] which is still too large for practical applications. It was predicted that J_c was proportional to M_s^2, α, and η^{-1} of the free layer,[13] where M_s is the saturation magnetization, α is the damping constant, and η is the spin polarization factor. Heusler alloys with lower M_s, smaller α, and higher spin polarization factor η are excellent candidates for reducing J_c compared with CoFe, Fe, Co, and Py.

Recently, smaller critical current J_c was indeed reported in spin-valve nanopillars with half-metallic Heusler alloys. Aoshima *et al.*[14] observed experimentally that J_c of Co_2MnGe, Co_2FeSi, and $Co_{75}Fe_{25}$ spin-valves were 1.6×10^7, 2.7×10^7, and 5.1×10^7 J/m^3, respectively. Furubayashi *et al.*[15] found a large magnetoresistance ratio of 6.9% at room temperature (RT) for $Co_2FeAl_{0.5}Si_{0.5}$ (CFAS)/Ag/CFAS spin-valves. Sukegawa *et al.*[16] showed that the resistance-current curves of $Co_2FeAl_{0.5}Si_{0.5}$ spin-valves exhibited a two-step switching process, which is similar to the behavior of the Fe/Ag/Fe nanopillar[17] and originated from the interplay between the magnetocrystalline anisotropy of CFAS layers and STT. Unlike most cases, for both $Co_2FeAl_{0.5}Si_{0.5}$ and Fe/Ag/Fe spin-valves it is believed that there exists an intermediate (I) state, besides the parallel (P) and antiparallel (AP) spin configurations, with the direction of the spins perpendicular to their original and final states when an appropriate negative current is applied. The magnetization reversal from the initial state (P) to the intermediate state (I) and then to the antiparallel state (AP) forms a two-step shape in the negative part of the hysteretic loop as the current increases. However, for a positive current, there is only one-step switching, i.e., the magnetization reversal from AP to P directly. The experimental result showed that the switching from P to I was gradual and I to AP was abrupt. It was hypothesized that those two switching processes were caused by different switching mechanisms.[16] The detailed features and full understanding of the switching mechanism of Heusler alloy spin-valves call for further investigations.

In this paper, we investigated spin-transfer switching of $Co_2FeAl_{0.5}Si_{0.5}$ (CFAS) alloy by using micromagnetic simulations. A two-step spin-transfer switching arising from the fourfold in-plane magnetocrystalline anisotropy was obtained in our simulations. The switching was accomplished through the domain wall motion. The critical current density J_c is 9.0×10^6A/cm^2, consistent with the experimental value of 9.3×10^6A/cm^2.[16] Furthermore, the switching time was discussed and the mechanism of spin-transfer switching was elucidated based on the magnetization trajectory and magnetization distribution.

II. THEORETICAL MODEL

As shown in Fig. 1, we studied a spin-valve device with geometry similar to the structure of the spin-valve in Ref. 16 [CFAS (20 nm)/Ag (4 nm)/CFAS (2.5 nm) of elliptical cross-section area (250×190 nm^2)]. We employ a Cartesian coordinate system where the x-axis is the long axis of the ellipse along the CFAS [110] direction (easy axis) and the y-axis is along the short axis ([1 $\bar{1}$ 0]). The magnetization

a)Author to whom correspondence should be addressed. Electronic mail: xqma@sas.ustb.edu.cn.

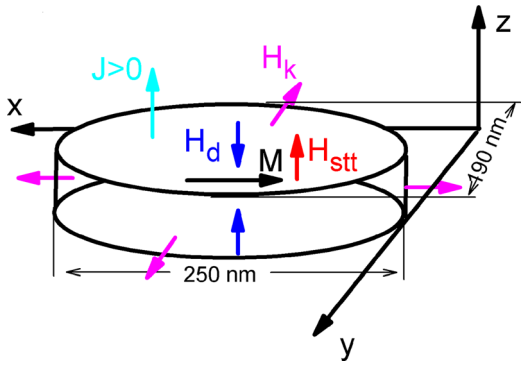

FIG. 1. (Color online) Model geometry definition of CFAS nanopillar in Cartesian coordinates for different contributions of magnetocrystalline anisotropic field $\mathbf{H}_k$, demagnetization field $\mathbf{H}_d$, and spin-transfer torque $\mathbf{H}_{stt}$ on the free layer.

dynamics are described using a generalized Landau-Lifshitz-Gilbert-Slonczewski (LLGS) equation,[1,2] which can be written as

$$\frac{d\mathbf{M}}{dt} = -\gamma'\mathbf{M}\times\mathbf{H}_{eff} - \frac{\alpha\gamma'}{M_s}\mathbf{M}\times(\mathbf{M}\times\mathbf{H}_{eff}) - \frac{2\mu_B J}{(1+\alpha^2)edM_s^3} \times g(\mathbf{M},\mathbf{P})\mathbf{M}\times(\mathbf{M}\times\mathbf{P}) + \frac{2\mu_B\alpha J}{(1+\alpha^2)edM_s^2}g(\mathbf{M},\mathbf{P})(\mathbf{M}\times\mathbf{P}) \quad (1)$$

where $\mathbf{M}$ is the magnetization of the free layer, $\mathbf{P}$ is the magnetization of the pinned layer, $\mathbf{H}_{eff}$ is the effective field, $\gamma' = \gamma/(1+\alpha^2)$, γ is the electron gyromagnetic ratio, and α is the dimensionless damping parameter. The effective field includes the anisotropy field, the demagnetization field, the external field, and the exchange field, namely $\mathbf{H}_{eff} = \mathbf{H}_k + \mathbf{H}_d + \mathbf{H}_{ext} + \mathbf{H}_{ex}$. Regarding the STT term, μ_B, J, d, e, and M_s are the Bohr magneton, the current density, the thickness of the free layer, the electron charge, and the saturation magnetization, respectively. The scalar function[1] $g(\mathbf{M}, \mathbf{P})$ is given by $g(\mathbf{M}, \mathbf{P}) = [-4 + (1+\eta)^3(3 + \mathbf{M}\cdot\mathbf{P}/M_s^2)/4\eta^{3/2}]^{-1}$, where the angle between $\mathbf{M}$ and $\mathbf{P}$ is θ. $\mathbf{M}\cdot\mathbf{P}/M_s^2 = \cos\theta$.

The positive current is generally defined as electrons flowing from the free layer to the pinned layer. The magnetic parameters are adopted[16] as follows: saturation magnetization $M_s = 9.0\times10^5$A/m, exchange constant $A = 2.0\times10^{-11}$J/m, Gilbert damping parameter $\alpha = 0.01$, spin polarization factor $\eta = 0.76$, and magnetocrystalline anisotropy constant $K_1 = -1.0\times10^4$ J/m^3. The initial magnetizations of free and pinned layers are along the $-$x axis and $+$x axis, respectively. The dynamics of magnetization were investigated by numerically solving the time-dependent LLGS equation using the Gauss-Seidel projection method[18–21] with a constant time step $\Delta t = 0.0238993$ ps. Simulations with a shorter time step gave the same results exactly. The samples were discrete, in computational cells of $2.5\times2.5\times2.5$ nm^3.

III. RESULTS AND DISCUSSION

We simulated the resistance as a function of current density (R-J) and qualitatively captured the major features of a two-step spin-transfer switching behavior as measured experimentally.[16] This two-step switching only exists in the negative current range, while one-step switching appears in the positive current range, as shown in Fig. 2(a). For dc current, the simulated switching current density is of the order of 10^6A/cm^2, which is consistent with the experiment value of 9.3×10^6A/cm^2.[16] In the R-J curves, three states are evident: the parallel (P), antiparallel (AP), and intermediate (I: perpendicular to $\mathbf{P}$) states. For one-step switching, the magnetization flips from P to AP under the driving of a sufficiently positive current with a threshold current of 24.0×10^6A/cm^2. For the two-step switching, the magnetization flip from AP to I occurs first, under the driving of a smaller negative polarized current 4.0×10^6A/cm^2. Then, it switches from I to P under a larger negative current 9.0×10^6A/cm^2. Another characteristic of the hysteretic loop is that the switching from AP to I is not as abrupt as the switching from I to P in the negative current direction. These characteristics of the hysteretic loop can be elucidated by Slonczewski's model,[1] which takes into account the interface spin-flip scattering between the layers. In this model, the relationship of STT versus θ is not symmetrical about 90°. STT reaches its maximum value at an angle of about 162°, as plotted in Fig. 2(b). This causes the special switching feature of the loop for the CFAS spin valve.

The characteristics of the switching and hysteresis loop of the CFAS spin valve can be explained as follows: whether it takes one-step or two-step switching depends on the interplay between STT and magnetocrystalline anisotropy. In the positive current density of 30.0×10^6A/cm^2, the effective field of the STT, $\mathbf{H}_{stt} = 2\mu_B Jg(\mathbf{M},\mathbf{P})/(\gamma edM_s^3)$ equals to 3.05×10^4 A/m at 90°, which is larger than the

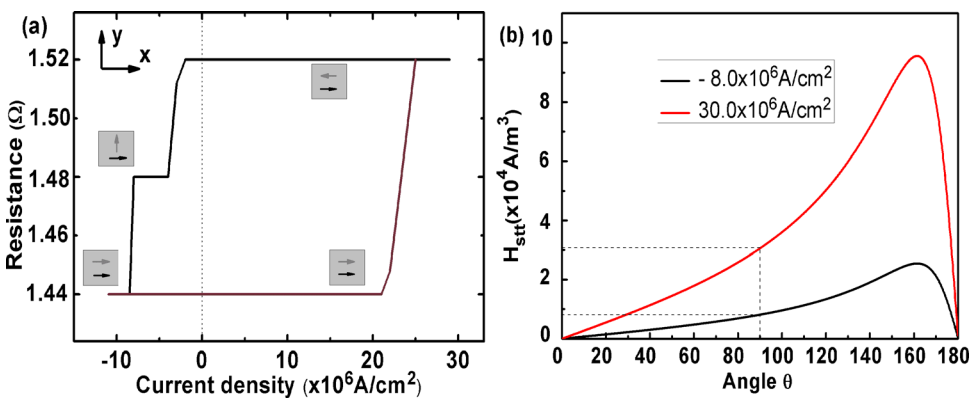

FIG. 2. (Color online) (a) Micromagnetic simulation of the resistance as a function of current density (R-J) curves of CFAS/Ag/CFAS CPP-GMR nanopillar. (b) The relationships of STT vs θ in Slonczewski's model.

magnetocrystalline anisotropy field of 1.18×10^4 A/m at the same angle. Therefore, $\mathbf{H}_{stt}$ can overcome the barrier of the magnetocrystalline anisotropy field and drive the magnetization switching from $\theta = 0°$ to 162°, where the STT reaches its maximum. After that, $\mathbf{H}_{stt}$ is always larger than the magnetocrystalline anisotropy field, since $\mathbf{H}_{stt}$ decreases as θ increases from 162° to 180°, making the magnetization switch to AP. Thus, the magnetization switching in a positive current is one-step switching. However, when a negative current is applied, if its magnitude is smaller than a threshold J_{c1}, the $\mathbf{H}_{stt}$ is too small to overcome the magnetocrystalline anisotropy torque. So, the magnetization does not switch but usually precesses. If the magnitude of the current is larger than J_{c1} but smaller than another threshold J_{c2}, $\mathbf{H}_{stt}$ increases as the direction of the magnetization gets farther away from 180°, and reaches a maximum at 162°. After that, the STT starts to decrease. At a 90° angle, $\mathbf{H}_{stt}$ is smaller than the magnetocrystalline anisotropy field, and it gets smaller and smaller as θ turn to 0. Therefore, STT cannot overcome the magnetocrystalline anisotropy barrier, leading to the magnetization stabilizing at the I state ($\theta = 90°$). For example, when the current density is -8.0×10^6 A/cm^2, $\mathbf{H}_{stt}$ is 0.85×10^4 A/m at 90°, smaller than the magnetocrystalline anisotropy field 1.17×10^4 A/m. If the magnitude of the negative current is greater than J_{c2}, in this case, $\mathbf{H}_{stt}$ is large enough to overcome the barrier of magnetocrystalline anisotropy. Therefore the magnetization can be switched from AP to P. The J_{c1} and J_{c2} values in this CFAS spin-valve simulation turn out to be 4.0×10^6 A/cm^2 and 9.0×10^6 A/cm^2, which are consistent with the experimental results.[16]

Focusing on the magnetization switching behavior, the experiment[16] showed that the shapes of the R-I curves did not change significantly as the external magnetic field increased from −10 to 20 Oe, only simply shifting in the positive direction. In our simulation, we obtained the same shape of the R-J curve without the external magnetic field. Our previous paper[21] showed that the external magnetic field can enormously affect the magnetization switching and critical current, either favoring or impeding the magnetization switching depending on its magnitude. The P state was no longer stable below −10 Oe and the AP state was not observed above 20 Oe in the experiment. That means the external magnetic field has an effect on the spin transfer switching, driving the magnetization to switch directly to the field direction. In addition, the size of the nanopillar also plays an important role in the magnetization switching behavior. There is a roughly linear increase in the critical current with the increase in size, as shown in Ref. 22, except in the range below a critical dimension, at which the magnetization structure is a single domain.

Furthermore, the switching from AP to I is slower than the switching from I to P. The difference of the switching times for these two processes originated from the different magnitudes of $\mathbf{H}_{stt}$ before switching, rather than different mechanisms. Because the magnitude of $\mathbf{H}_{stt}$ for $\theta = 90°$ is larger than that for $\theta = 0°$ and 180°, the switching time from I to P is shorter than that from AP to I. Additionally, $\mathbf{H}_{stt}$ at the current density of -4.0×10^6 A/cm^2 is smaller than that of -8.0×10^6 A/cm^2 since $\mathbf{H}_{stt}$ is proportional to the current density.

Figures 3(a) and 3(b) show temporal evolutions of the average normalized magnetization components $\langle m_x \rangle$, $\langle m_y \rangle$, and $\langle m_z \rangle$ ($\mathbf{m} = \mathbf{M}/M_s$) at the current densities of -8.0×10^6 A/cm^2 and -70.0×10^6 A/cm^2, respectively. The spin-transfer switching is accompanied by drastic magnetization oscillation. The amplitude of $\langle m_z \rangle$ oscillation is very small. This is because the size of the free layer in the z direction (2.5 nm) is significantly smaller than those of the x and y directions (250 nm × 190 nm), resulting in much stronger demagnetization fields in the z direction. Therefore, the higher demagnetization field in the z direction impedes the development of $\langle m_z \rangle$. Figures 3(c) and 3(d) are the

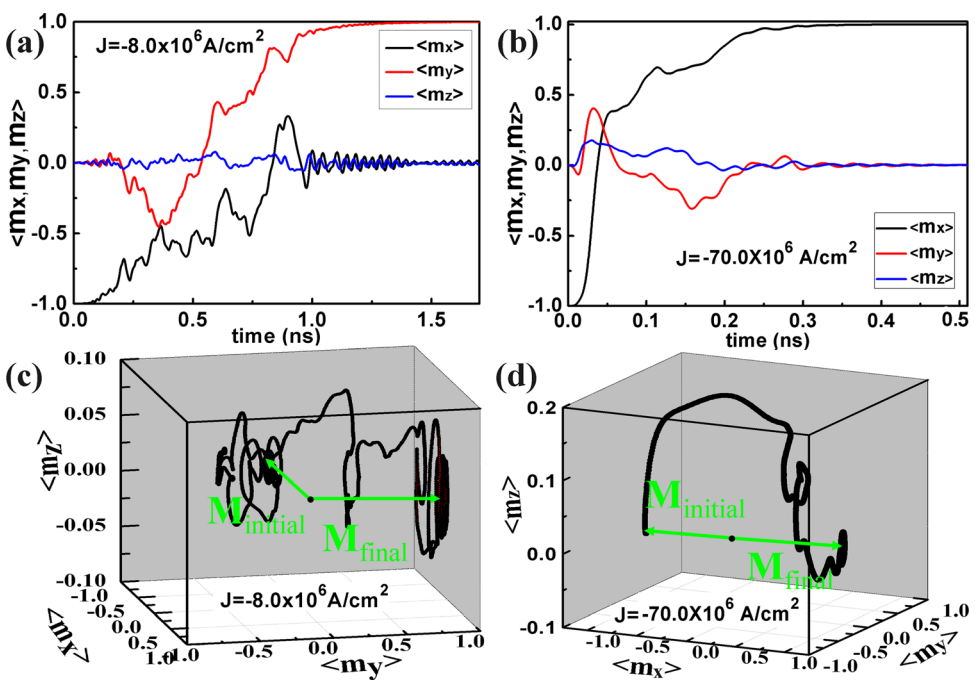

FIG. 3. (Color online) The temporal evolutions of $\langle m_x \rangle$ (black), $\langle m_y \rangle$ (red), and $\langle m_z \rangle$ (blue) under the current densities of (a) -8.0×10^6 A/cm^2 and (b) -70.0×10^6 A/cm^2. The magnetization trajectories from the initial state ($\mathbf{M}_{initial}$) to the final state ($\mathbf{M}_{final}$) under the current densities of (c) -8.0×10^6 A/cm^2 and (d) -70.0×10^6 A/cm^2.

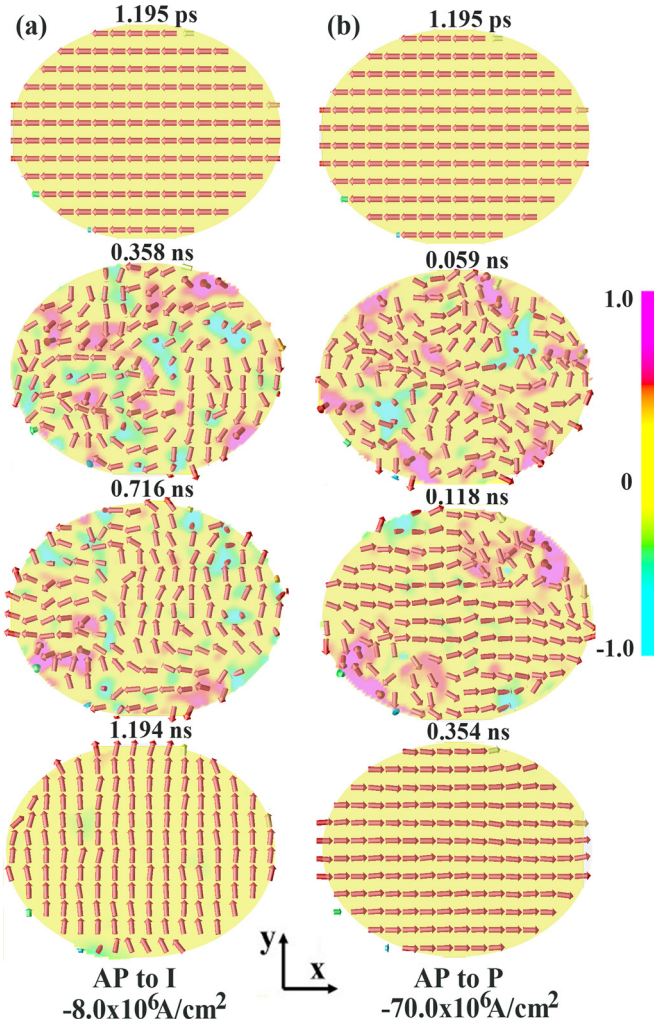

FIG. 4. (Color online) Snapshots of magnetization distribution of the 250×190 nm^2 ellipse. The colors represent the average magnetization component of $<m_z>$ (red positive, cyan negative). (a) -8.0×10^6 A/cm^2. (b) -70.0×10^6 A/cm^2.

magnetization switching trajectories[23,24] from AP to I at the current density of -8.0×10^6A/cm^2 and from AP to P at the current density of -70.0×10^6A/cm^2. In those switching regions, STT excites coherent precession that eventually leads to magnetization switching from the initial state ($\mathbf{M}_{\text{initial}}$) to the final state ($\mathbf{M}_{\text{final}}$). The anisotropy energy barriers to overcome in both those switching cases are the same, but the different magnitudes of $\mathbf{H}_{stt}$ result in two switching speeds. The switching times for two current densities are 1.4 ns and 0.4 ns, respectively. The predicted relationship between current density and switching time can potentially be used for the design of STT-MRAM devices.

We also simulated the time-dependent magnetization distribution for negative current densities, which are similar to prior works using the free layers of Co and CoFeB.[24,25] Fig. 4 shows snapshots of the main steps of spin-transfer switching from AP to I (or P) for a 250×190 nm^2 ellipse. The magnetization switches to the y axis (AP to I) at the current density of -8.0×10^6 A/cm^2, while the magnetization switches to the x axis (AP to P) at the current density -70.0×10^6 A/cm^2. The colors represent the average magnetization components of $<m_z>$. The magnetization at each point of the free layer experiences a torque exerted by the STT, with its magnitude being decided by the angle between **M** and **P**. This means that $\mathbf{H}_{stt}$ is the largest when the angle θ is close to 162°. $\mathbf{H}_{stt}$ is zero when the angle θ is 0° or 180°. The major part of the magnetization of the free layer is close to parallel or antiparallel to the **P** (+x direction) except near the domain wall area. The angle between the magnetization at the domain wall and **P** varies from 0° to 180°, so the moments in the domain walls will experience the biggest torque by the STT, far greater than those within the domains. This drives the domain wall motion and facilitates the domain switching. The switching is first excited at the boundaries of the structure via the nucleation process because of spatially non-uniform local demagnetizing fields.[22,25] Then they expand to the center of the structure, with the reversal domains enlarged by STT, causing the formation of multi-domains. At the end, the magnetization finishes the switches process from AP to I or AP to P.

IV. CONCLUSIONS

In conclusion, we investigated the spin-transfer switching in a full-Heusler $Co_2FeAl_{0.5}Si_{0.5}$ (CFAS) alloy spin-valve nanopillar using micromagnetic simulations. We predicted a two-step switching due to the fourfold in-plane magnetocrystalline anisotropy of CFAS layers in the negative current range, which is consistent with the experimental R-J curve, while only one-step switching appears in the positive current range. The switching from AP to I is slower than the switching from I to P in the negative current direction caused by the different magnitudes of $\mathbf{H}_{stt}$, rather than different mechanisms. These two characteristics were explained by Slonczewski's model. Furthermore, we analyzed the two-step switching process and its mechanism in a spin-transfer switching of a full-Heusler $Co_2FeAl_{0.5}Si_{0.5}$ spin-valve nanopillar using the magnetization distributions and trajectories.

ACKNOWLEDGMENTS

This work was sponsored by the National Science Foundation of China (5042810) and by the US National Science Foundation under the grant number DMR-1006541 (Chen).

[1]J. C. Slonczewski, J. Magn. Magn. Mater. **159**, L1 (1996).
[2]L. Berger, Phys. Rev. B **54**, 9359 (1996).
[3]E. B. Myers, D. C. Ralph, J. A. Katine, R. N. Louie, and R. A. Buhrman, Science **285**, 867 (1999).
[4]J. A. Katine, F. J. Albert, R. A. Buhrman, E. B. Myers, and D. C. Ralph, Phys. Rev. Lett. **84**, 3149 (2000).
[5]M. Tsoi, A. G. M. Jansen, J. Bass, W. C. Chiang, M. Seck, V. Tsoi, and P. Wyder, Phys. Rev. Lett. **80**, 4281 (1998).
[6]S. I. Kiselev, J. C. Sankey, I. N. Krivorotov, N. C. Emley, R. J. Schoelkopf, R. A. Buhrman, and D. C. Ralph, Nature **425**, 380 (2003).
[7]Y. Jiang, S, Abe, T. Ochiai, T, Nozaki, A. Hirohata, N. Tezuka, and K. Inomata, Phys. Rev. Lett. **92**, 167204 (2004).
[8]Y. Jiang, T, Nozaki, S, Abe, T. Ochiai, A. Hirohata, N. Tezuka, and K. Inomata, Nature Mater. **3**, 1 (2004).
[9]P. M. Braganca, I. N. Krivorotov, O. Ozatay, A. G. F. Garcia, N. C. Emley, J. C. Sankey, D. C. Ralph, and R. A. Buhrman, Appl. Phys. Lett. **87**, 112507 (2005).
[10]C. Yen, W. Chen, D. Wang, Y. Lee, C. Shen, S. Yang, C. Tsai, C. Hung, K. Shen, M. Tsai, and M. Kao, Appl. Phys. Lett. **93**, 092504 (2008).

[11]H. Kubota, A. Fukushima, K. Yakushiji, S. Yakata, S. Yuasa, K. Ando, M. Ogane, Y. Ando, and T. Miyazaki, J. Appl. Phys. **105**, 07D117 (2009).
[12]L. Liu, T. Moriyama, D. C. Ralph, and R. A. Buhrman, Appl. Phys. Lett. **94**, 122508 (2009).
[13]J. Z. Sun, Phys. Rev. B **62**, 570 (2000).
[14]K. Aoshima, N. Funabashi, K. Machida, Y. Miyamoto, K. Kuga, and N. Kawamura, J. Magn. Magn. Mater. **310**, 2018 (2007).
[15]T. Furubayashi, K. Kodama, H. Sukegawa, Y. K. Takahashi, K. Inomata, and K. Hono, Appl. Phys. Lett. **93**, 122507 (2008).
[16]H. Sukegawa, S. Kasai, T. Furubayashi, S. Mitani, and K. Inomata, Appl. Phys. Lett. **96**, 042508 (2010).
[17]R. Lehndorff, M. Buchmeier, D. E. Bürgler, A. Kakay, R. Hertel, and C. M. Schneider, Phys. Rev. B **76**, 214420 (2007).
[18]X. P. Wang, C. J. García-Cervera, and E. Weinan, J. Comput. Phys. **171**, 357 (2001).
[19]J. X. Zhang and L. Q. Chen, Acta Mater. **53**, 2845 (2005).
[20]Z. H. Xiao, X. Q. Ma, P. P. Wu, J. X. Zhang, L. Q. Chen, and S. Q. Shi, J. Appl. Phys. **102**, 093907 (2007).
[21]X. Q. Ma, Z. H. Xiao, P. P. Wu, J. X. Zhang, L. Q. Chen, and S. Q. Shi, J. Appl. Phys. **103**, 07B111 (2008).
[22]R. Heindl, S. E. Russek, T. J. Silva, W. H. Rippard, J. A. Katine, and M. J. Carey, Appl. Phys. Lett. **92**, 262504 (2008).
[23]J. Guo, M. B. A. Jalil, and S. G. Tan, Appl. Phys. Lett. **92**, 182103 (2008).
[24]D. V. Berkov and N. L. Gorn, Phys. Rev. B **71**, 052403 (2005).
[25]K. J. Lee, A. Deac, O. Redon, J. P. Nozieres, and B. Dieny, Nature Mater. **3**, 877 (2004).